

## PULSED LASER DEPOSITION OF NOVEL HTS MULTILAYERS FOR PASSIVE AND ACTIVE DEVICE APPLICATIONS,

D.B. Chrisey, J.S. Horwitz, J.M. Pond, K.R. Carrol, P. Lubitz, K.S. Grabowski, R.E. Leuchtner, and C.A. Carosella  
Naval Research Laboratory, Washington, D.C. 20375

and

C.V. Vittoria  
Northeastern University, Boston, MA 02115

*Abstract*-- Multilayered structures have been fabricated from binary combinations of the high  $T_c$  superconductor  $YBa_2Cu_3O_{7-\delta}$  (YBCO) and the ferrite  $BaFe_{12}O_{19}$  (BFO) or the ferroelectric  $Sr_{0.5}Ba_{0.5}TiO_3$  (SBT). The combination of YBCO and BFO was found to destroy the superconductivity of the YBCO layer. Vibrating sample magnetometer measurements of the BFO layer still indicated a large uniaxial anisotropy. The underlying YBCO layer, of an SBT/YBCO bilayer still had high quality transport properties unaffected by the SBT layer ( $T_c \sim 91$  K,  $J_c(77$  K)  $\sim 2 \times 10^6$  A/cm<sup>2</sup>). A thin film, normal metal/SBT transmission line, patterned in microstrip, demonstrated a wealth of temperature and electric field dependent dielectric information for the frequency range tested ( $f \leq 3$  GHz). At 100 K, the dielectric constant for zero applied field was 250 for frequencies less than 30 MHz; it was  $\sim 120$  for  $1$  GHz  $\leq f \leq 3$  GHz, and it varied continuously with frequency between these values. For temperatures between 300 K and 11 K, frequencies less than about 0.5 GHz, and applied fields up to 200 kV/cm, a nearly linear change in field-induced phase difference was produced in the transmission line. Above this frequency the field dependence changed sign and essentially disappeared at  $\sim 1$  GHz.

### I. INTRODUCTION

The first generation of high temperature superconductor (HTS) multilayers were composed of layers of HTS (typically  $YBa_2Cu_3O_{7-\delta}$ ) and common lattice-matched insulators (e.g.,  $LaAlO_3$  or  $PrBa_2Cu_3O_7$ ). Their choice was governed by the ability to maintain epitaxy and to separate electrically the  $YBa_2Cu_3O_{7-\delta}$  (YBCO) layers for waveguide or junction applications, respectively. Second generation dielectrics in HTS multilayers will likely support a more useful function than simply dielectric slowing, e.g., actively changing the permittivity in response to a moderate electric field.

Thin film heterostructures made from HTS and ferrites and ferroelectrics offer unique opportunities for the fabrication of advanced microwave circuit elements. Based on bulk and single layer thin films these structures were predicted to have novel physical properties as a result of the interaction of the component materials. Recently, it was shown in bulk  $Sr_{0.5}Ba_{0.5}TiO_3$  (SBT) that electric fields of 20 kV/cm could change the dielectric constant by as much as 54% [1]. For applications such as phase shifters these bulk materials would require  $\sim 1000$  volts to achieve useable phase shift. Assuming that thin film properties could be extrapolated from bulk behavior, a 1  $\mu$ m thick film would only require a bias of  $\sim 10$

volts. This is a much more realistic value to be obtained and applied in a T/R module phase shifter. In addition, the combination of SBT with YBCO would be especially appropriate for maintaining crystalline epitaxy and low insertion losses.

Combining thin films of  $BaFe_{12}O_{19}$  (BFO) with YBCO should show novel external flux pinning properties, assuming again that bulk behavior extrapolates to thin film form. These properties would be a result of the interaction of the component materials at the interface. For a BFO/YBCO bilayer, magnetic domains in BFO layer would exceed  $H_{c1}$  and induce fluxoids in the YBCO film. The energy required to cause flux flow would then be the sum of the conventional pinning energy and the additional energy required to move the domain walls (external to the YBCO layer). This, in effect, causes additional pinning strength, and thus, higher thin film critical currents.

We have deposited novel multilayers of ferrites ( $BaFe_{12}O_{19}$ ) and ferroelectrics ( $Sr_{0.5}Ba_{0.5}TiO_3$ ) with  $YBa_2Cu_3O_{7-\delta}$ . The goal of this work was to determine whether bulk and single layer properties could easily be transferred to thin film multilayers and to explore the aforementioned applications. The pulsed laser deposition approach seemed especially appropriate for this investigation since all that is required to deposit multilayers is to change the targets. Also our group has previously demonstrated the ability to deposit separately all of the classes of materials proposed, and to pattern HTS devices and HTS multilayers [2-8].

### II. EXPERIMENT

The pulsed laser deposition system used for multilayer preparation has been described previously [2]. Briefly, the focussed output of a KrF excimer laser was used to ablate stoichiometric targets of  $YBa_2Cu_3O_{7-\delta}$  (YBCO), and either  $BaFe_{12}O_{19}$  (BFO) or  $Sr_{0.5}Ba_{0.5}TiO_3$  (SBT). The electrical and structural transport properties of single layer  $YBa_2Cu_3O_{7-\delta}$  was optimized at 750°C and 300 mTorr of oxygen. The optimum conditions for pulsed laser depositing single layers of  $BaFe_{12}O_{19}$  were 900°C and 400 mTorr of oxygen on  $\langle 0001 \rangle$   $Al_2O_3$ . Details of single film properties have been published elsewhere [4]. In some cases, an oriented Pt layer was used as a chemically inert conducting layer when characterizing the ferroelectrics. For these cases it has been found that deposition at 450°C in 50 mTorr of argon onto  $\langle 100 \rangle$  MgO results in  $\langle 100 \rangle$  oriented Pt [6]. The  $Sr_{0.5}Ba_{0.5}TiO_3$  was deposited at 750°C in 300 mTorr of oxygen. It is not known whether

these conditions are optimum for the deposition of  $\text{Sr}_{0.5}\text{Ba}_{0.5}\text{TiO}_3$  single or bilayers.

### III. RESULTS

#### A. HTS/Ferrite Multilayer Results

The BFO/YBCO multilayers were grown in both orders, i.e., the YBCO layer was grown first and then the BFO layer and vice versa. But two different substrates were used, depending on order, to optimize the oriented growth of the bottom layer.  $\langle 100 \rangle$  MgO was used as a substrate for YBCO and  $\langle 0001 \rangle$   $\text{Al}_2\text{O}_3$  was used for BFO. When YBCO was deposited first, and before the BFO layer was deposited, the transport properties were measured and found to be high quality. In all cases, the resulting combination of BFO and YBCO caused the YBCO layer to be nonsuperconducting for temperatures above 4.2 K. The hysteresis curves for the BFO indicated the ferrite layer was not similarly destroyed.

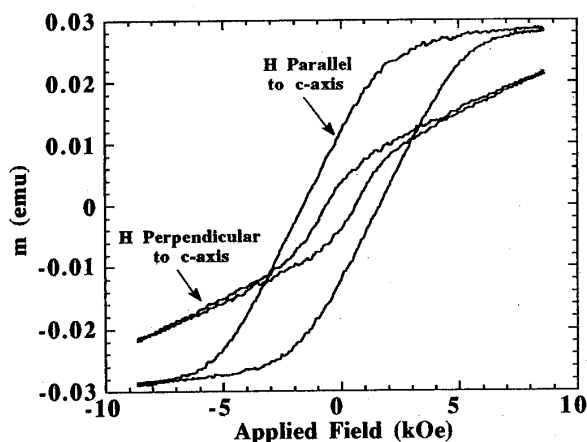


Fig. 1 Hysteresis curves for a YBCO/BFO bilayer on a  $\langle 0001 \rangle$   $\text{Al}_2\text{O}_3$  substrate. The two curves are for the field applied perpendicular and parallel to the c-axis.

In Fig. 1 we present the vibrating sample magnetometer hysteresis curves for a YBCO/BFO bilayer on a  $\langle 0001 \rangle$   $\text{Al}_2\text{O}_3$  substrate [9]. The two curves are for the field applied perpendicular and parallel to the c-axis. A large uniaxial anisotropy is observed consistent with c-axis texturing in the BFO layer. The perpendicular coercivity  $H_c$  and anisotropy field  $H$ , are 0.6 and 17 kOe, respectively. Qualitatively similar results were found for the bilayer deposited in the opposite order, i.e., with the YBCO deposited first, with the only difference being slightly less uniaxial anisotropy. Similar results were obtained by Naoe et al. for sputtered bilayers [9]. X-ray diffraction analysis of the c-axis lattice parameter suggested the superconductivity was destroyed in the YBCO layer by the extraction of oxygen from the YBCO layer. Auger depth profile showed no apparent interdiffusion. It is possible that the use of appropriate buffer layers in the future could mitigate this problem.

#### B. HTS/Ferroelectric Multilayer Results

We have successively deposited oriented bilayers of SBT and YBCO. In Fig. 2 we show the x-ray diffraction pattern for SBT/YBCO on an  $\langle 100 \rangle$  MgO substrate. This pattern indicates the SBT film contained both  $\langle 100 \rangle$  oriented grains (with a rocking curve width of  $\sim 0.8^\circ$ ) and some randomly oriented grains of SBT. It is possible that the initial epitaxy was lost as the film became thicker. The electrical transport properties of the YBCO layer were measured inductively after the SBT deposition and found to be  $T_c \sim 91$  K and  $J_c(77$  K)  $\sim 2 \times 10^6$  A/cm $^2$ .

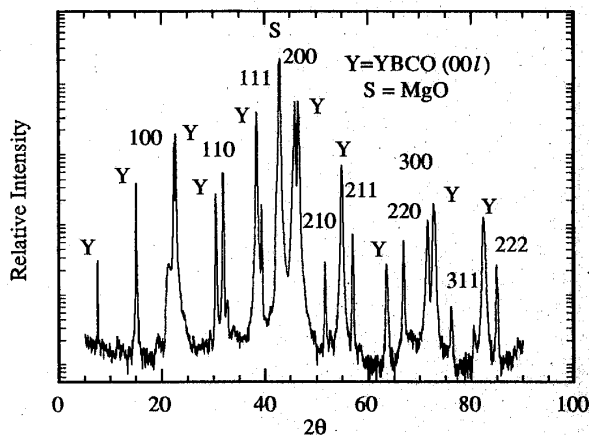


Fig. 2 The x-ray diffraction spectrum of SBT/YBCO on an MgO substrate.

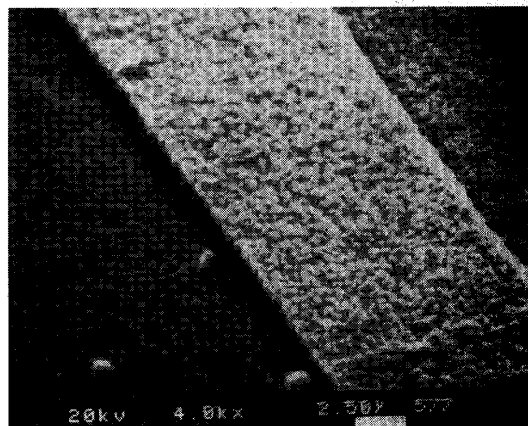


Fig. 3 SEM image of the 12  $\mu\text{m}$  wide by 1 cm long Ag transmission line used to characterize the dielectric constant of the SBT layer at microwave frequencies. The length bar is 2.5  $\mu\text{m}$ .

Expecting similar degradation of the YBCO layer as was found with the BFO ferrites, we also deposited SBT onto an MgO substrate coated with 1  $\mu\text{m}$  of epitaxial  $\langle 100 \rangle$  Pt. The x-ray diffraction pattern for the SBT film on Pt indicated

$\langle 110 \rangle$  preferential orientation (instead of  $\langle 100 \rangle$ ) was present. Less randomly oriented material was observed.

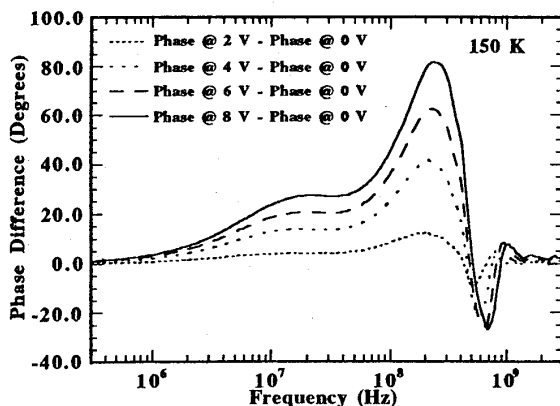


Fig. 4 The phase difference observed at 150 K versus frequency for various applied fields.

The SBT/Pt on MgO bilayer was used to characterize the field and temperature dependence of the SBT's dielectric constant. On top of the SBT a 12  $\mu\text{m}$  wide by 1 cm long by 1  $\mu\text{m}$  thick Ag transmission line was e-beam deposited and photolithographically patterned. In this case, the SBT layer was 4000  $\text{\AA}$  thick (see Fig. 3). Microwave signals were transmitted through this microstrip device and  $S_{21}$  was analyzed on an HP 8753A vector network analyzer. In Fig. 4 we plot the phase difference observed at 150 K versus frequency for various applied fields. The qualitative features of this plot were similar for all temperatures measured between 11 K and 300 K. Fig. 4 shows that the application of an electric field can cause additional phase shift, at any given frequency ( $f < 0.5$  GHz), similar to what is observed in bulk SBT and that the magnitude of phase change increases monotonically with frequency for  $f < 0.5$  GHz. What is not clear from this plot is that the dielectric constant is changing as a function of frequency. Also, the physical causes for the peaks and the rapid change in behavior between 0.5 GHz and 1 GHz are not understood.

Assuming a parallel plate geometry the dielectric constant was calculated at 100 K at several frequencies. For frequencies less than 30 MHz the dielectric constant was 250. For frequencies between 1 and 3 GHz the value was 120. The dielectric constant varied continuously between these values. The DC resistance through the dielectric of the device was greater than 0.5  $\text{M}\Omega$  throughout the temperature and voltage ranges explored. Taking into account the geometry, this translates to a resistivity greater than  $1.5 \times 10^7 \Omega\text{cm}$ .

As the temperature was varied between 11 K and 300 K the frequency and electric field dependence of the SBT's dielectric constant was modified. In Fig. 5 we plot the phase difference at 8 volts versus frequency for temperatures incremented by  $\sim 100$  K. What is evident from Fig. 5 is that the response is maximized near 200 K for almost the entire frequency range. From bulk work, it is expected that this response be maximized near the ferroelectric Curie temperature,

which is where the dielectric susceptibility changes from ferroelectric to paraelectric behavior. For this composition the bulk Curie temperature was  $\sim 260$  K.

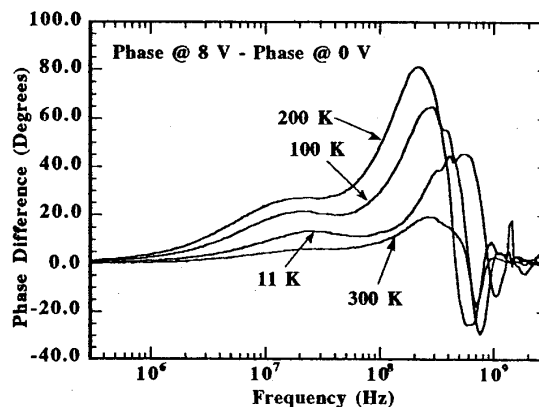


Fig. 5 Phase difference observed at 8 volts bias versus frequency for several temperatures. A bias of 8 volts corresponds to an electric field strength of 200 kV/cm.

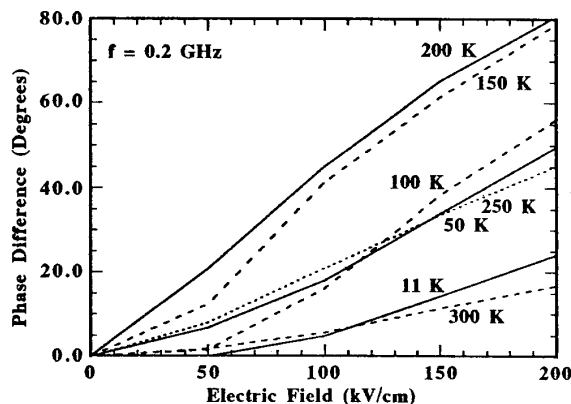


Fig. 6 Phase difference observed at 0.2 GHz versus applied electric field for each temperature measured.

In Fig. 6 we plot the phase difference observed at 0.2 GHz versus applied electric field for each temperature measured. At each temperature we observe a roughly linear change in phase with electric field. Also, the field-induced change in phase is maximized near 150 K to 200 K. It should be noted that the electric field strength used in this thin film device (200 kV/cm) is roughly an order of magnitude higher than that used by Varadan et al. and it is near the dielectric breakdown voltage of this material [1]. To better observe the temperature dependence of the field-induced change in phase we

linearly fit the data in Fig. 6 and plot the slope versus temperature. This data is shown in Fig. 7.

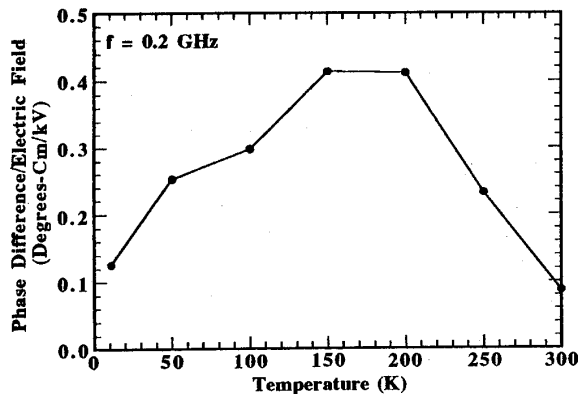


Fig. 7 Phase difference per electric field strength at 0.2 GHz versus temperature.

From Fig. 7 it is apparent that the Curie temperature for thin film SBT occurs between 150 K and 200K. This value is about 100 degrees lower than that observed in bulk SBT. The Curie temperature is known to be a strong function of the Sr to Ba doping varying from 110 K for SrTiO<sub>3</sub> to 408 K for BaTiO<sub>3</sub>. Rutherford backscattering analysis of the stoichiometry of this film indicated a Sr/Ti and Ba/Ti ratio of ~0.5, consistent with the pulsed laser deposition target stoichiometry.

#### IV. CONCLUSION

We have deposited novel multilayers of HTS and ferrites and ferroelectrics. While the BFO layer destroyed the superconductivity of the YBCO layer, in the YBCO/BFO bilayer, the BFO layer had acceptable properties. Thin insulating buffer layers could restore the superconductivity and improve the magnetic properties. The dielectric constant of the SBT transmission line showed extremely interesting electric field and temperature response, most of which is not understood. For SBT to be useful in an active microwave device it must remain electric-field-active until much higher frequencies.

#### REFERENCES

- [1] V.K. Varadan, D.K. Ghodgaonkar, V.V. Varadan, J.F. Kelly, and P. Glikerdas, "Ceramic Phase Shifters for Electronically Steerable Antenna Systems," *Microwave Journal*, pp. 116-127, January 1992.
- [2] D.B. Chrisey, J.S. Horwitz, H.S. Newman, M.E. Reeves, B.D. Weaver, K.S. Grabowski, and G.P. Summers, "Proton-induced reduction of  $R_s$ ,  $J_c$ , and  $T_c$  in YBa<sub>2</sub>Cu<sub>3</sub>O<sub>7- $\delta$</sub>  thin films," Vol. 4, pp. 57-60, 1991.
- [3] J.S. Horwitz, K.S. Grabowski, D.B. Chrisey, and R.E. Leuchtner, "In situ deposition of epitaxial PbZr<sub>x</sub>Ti<sub>(1-x)</sub>O<sub>3</sub> thin films by pulsed laser deposition," *Appl. Phys. Lett.*, Vol. 59, pp. 1565-1567, 1991.
- [4] C.A. Carosella, D.B. Chrisey, P. Lubitz, J.S. Horwitz, P. Dorsey, R. Seed, and C. Vittoria, "Pulsed laser deposition of epitaxial BaFe<sub>12</sub>O<sub>19</sub> thin films," *J. Appl. Phys.*, Vol. 71, pp. 5107-5110, 1992.
- [5] C.M. Williams, D.B. Chrisey, P. Lubitz, K.S. Grabowski, and C.M. Cotell, "The Magnetic Properties of Pulsed Laser Deposited Epitaxial Mn<sub>1-x</sub>Zn<sub>x</sub>Fe<sub>2</sub>O<sub>4</sub> Ferrite Films," Unpublished Data.
- [6] R.E. Leuchtner, D.B. Chrisey, J.S. Horwitz, and K.S. Grabowski, "The preparation of epitaxial platinum films by pulsed laser deposition," *Surf. and Coatings Tech.*, Vol. 51, pp. 476-482, 1992.
- [7] J.M. Pond, K.R. Carroll, J.S. Horwitz, D.B. Chrisey, M.S. Osofsky, and V.C. Cestone, "Penetration depth and microwave loss measurements with a YBa<sub>2</sub>Cu<sub>3</sub>O<sub>7- $\delta$</sub> /LaAlO<sub>3</sub>/YBa<sub>2</sub>Cu<sub>3</sub>O<sub>7- $\delta$</sub>  trilayer transmission line," *Appl. Phys. Lett.*, Vol. 59, pp. 3033-3035, 1991.
- [8] H.S. Newman, D.B. Chrisey, J.S. Horwitz, B.D. Weaver, and M.E. Reeves, "Microwave devices using YBa<sub>2</sub>Cu<sub>3</sub>O<sub>7- $\delta$</sub>  films made by pulsed laser deposition," *IEEE Trans. on Mag.*, Vol. 27, pp. 2540-2543, 1991.
- [9] M. Naoe, N. Matsushita, and S. Nakagawa, "Successive growth of Ba-ferrite magnetic layers on c-axis oriented YBaCuO superconductive layers," *J. Appl. Phys.*, Vol. 70, pp. 6489-6491, 1992.